

# Isothermal Crystallization of iPP in Model Glass-Fiber Composites

A. JANEVSKI,<sup>1</sup> G. BOGOEVA-GACEVA<sup>2</sup>

<sup>1</sup> Research Institute "OHIS," Skopje, Macedonia

<sup>2</sup> Faculty of Technology & Metallurgy, Skopje, Macedonia

Received 9 July 1997; accepted 29 December 1997

**ABSTRACT:** Isothermal crystallization of iPP in model glass-fiber composites is studied by DSC, and the basic energetic parameters of crystallization are determined. Unsized untreated and thermally treated glass fibers are used in model composites to determine the role of the surface on nucleation and crystallization processes. Thermally treated glass fibers are found to exhibit a predominant nucleating effect as compared to unsized untreated ones, and the crystallization proceeds faster, resulting in lower values for the half-time of crystallization (10–120 s). The energy of formation of a nuclei of critical dimensions at a given  $T_c$  is also lower, and it decreases as the content of the fibers in the composite increases. The surface free energy of folding,  $\sigma_e = 140 \times 10^{-3} \text{ J/m}^2$ , was determined for iPP in the composite containing 50% glass fibers, while for pure iPP,  $\sigma_e = 170 \times 10^{-3} \text{ J/m}^2$  was found. © 1998 John Wiley & Sons, Inc. *J Appl Polym Sci* 69: 381–389, 1998

**Key words:** iPP; glass fibers; model composites; isothermal crystallization; DSC

## INTRODUCTION

It is known that the presence of a solid surface (substrate) in contact with thermoplastic polymers during the crystallization from the melt generally favors the heterogeneous nucleation<sup>1,2</sup> and often a growth of the transcrystalline zone.<sup>3–5</sup> The specific morphology of the polymer in the transcrystalline zone is expected to influence the adhesion at the interface, due to an increased nucleation density as well as the mechanical properties of the interphase due to a preferential orientation of the lamellae.<sup>1</sup>

Transcrystallization is possible when the energetic parameters for nucleation on the surface (substrate) are favorable as compared to the bulk of the polymer.<sup>6,7</sup> For iPP, transcrystallization has been observed in the presence of crystalline/semicrystalline substrates, such as carbon fibers and

talc.<sup>8,9–12</sup> Numerous results are also reported on glass fiber/iPP composites concerning transcrystallization phenomena, many of them being conflicting. It was recently shown that the transcrystalline zone appeared only if the glass fiber is pulled out from the polymer melt or when shear stress is applied at given crystallization temperature.<sup>8,12,13</sup> On the other hand, although it has been found that the glass fiber increases the nucleation density,<sup>9</sup> the existence of a transcrystalline zone was not proved by microscopic investigations.<sup>9,14</sup>

This article is the second part of a study of model and bulk composites based on iPP and glass (or carbon) fibers, produced from knitted textile preforms of hybrid yarns.<sup>15</sup> In our previous article, the results on crystallization and fusion of textile-grade iPP, used for the processing of hybrid yarns and corresponding knitted fabrics, were reported.<sup>16</sup> The kinetics of crystallization of iPP in the dynamic and isothermal regime was followed by DSC, and the results were analyzed by Avrami, Ozawa, and Harnisch–Muschik methods. In this second part, the crystallization of iPP is analyzed by DSC in model

---

Correspondence to: G. Bogoeva-Gaceva.

*Journal of Applied Polymer Science*, Vol. 69, 381–389 (1998)  
© 1998 John Wiley & Sons, Inc.

CCC 0021-8995/98/020381-09

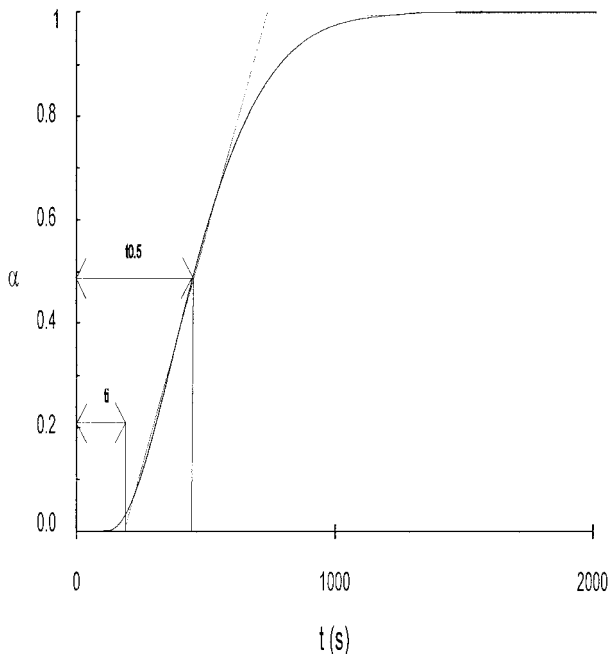


**Figure 1** Schematic diagram of crystal conversion ( $\alpha$ ) versus time ( $t$ ) with definition of induction time ( $t_i$ ) and half-time of crystallization ( $t_{0.5}$ ).

composites with glass fibers. When glass fibers are given thermal treatment, partial crystallization of the surface may be induced.<sup>17</sup> Mechanical properties of the fibers are decreased as a result of the creation of an uneven crystal structure on the surface of amorphous fibers. Energetic parameters of unsized untreated as well as thermally treated glass fibers were determined from the DSC data, in order to recognize the influence of surface treatment on the crystallization behavior and transcristallization phenomena.

## EXPERIMENTAL

Model composites were prepared by mixing chopped glass fibers (GF) with thin iPP film, previously prepared by melting the polymer at 473 K between two PTFE plates. For the preparation of the composites, untreated unsized (assigna-

tion: UGF), as well as thermally treated (assignment: TGF) glass fibers were used. Glass fibers (E-glass) (produced by OHIS, Skopje, Macedonia) with a nominal diameter of 13  $\mu\text{m}$  were first treated 5 min at 573 K and then 30–120 min at 773 K. Consequently, the mechanical properties of the fibers are decreased, due to the crystallization at the surface.<sup>17</sup> Fiber-grade iPP with an MFI of 230°C 12–14 g/10 min (Daplen MT 55 Pre-spatex) was first melted to obtain a thin-film specimen and then placed into the DSC sample pan. Over the film, the chopped glass fibers are added, and the sample is rapidly heated to 478 K and the molten state held for 5 min to erase the thermal history of the polymer. Then, the sample is cooled

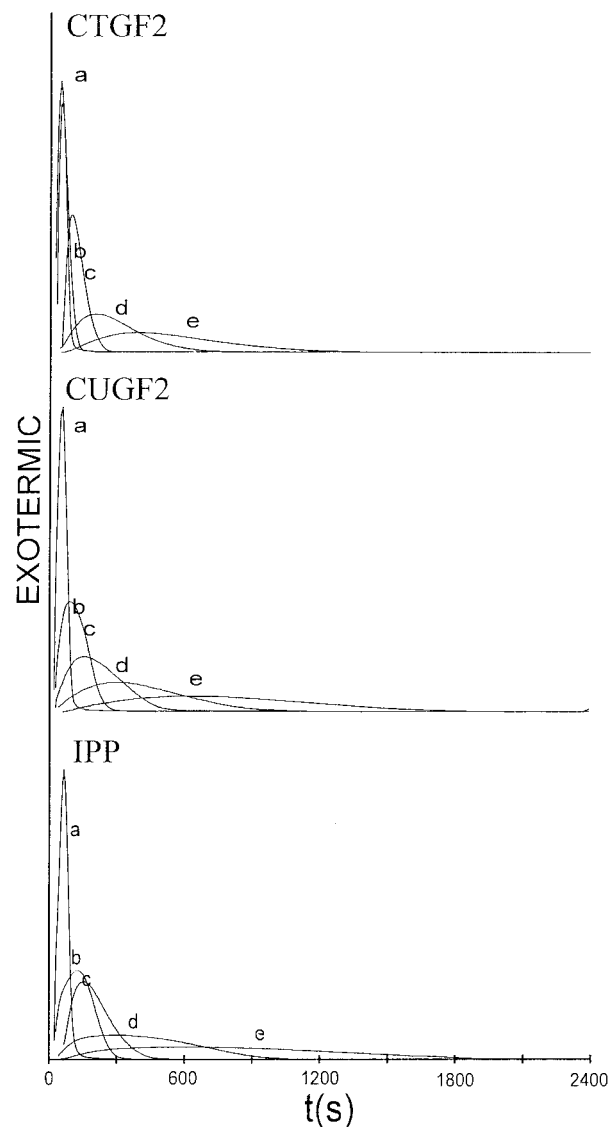


**Figure 2** DSC traces of isothermal crystallization for pure iPP and model composites carried out at  $T_c$ : (a) 388 K; (b) 391 K; (c) 394 K; (d) 397 K; (e) 400 K.

**Table I** Assignment of the Model Composites

GF Assignment	Content of GF (%)			
	0	20	30	50
TGF	iPP	CTGF2	CTGF3	CTGF5
UCF	iPP	CUGF2	CUGF3	CUGF5

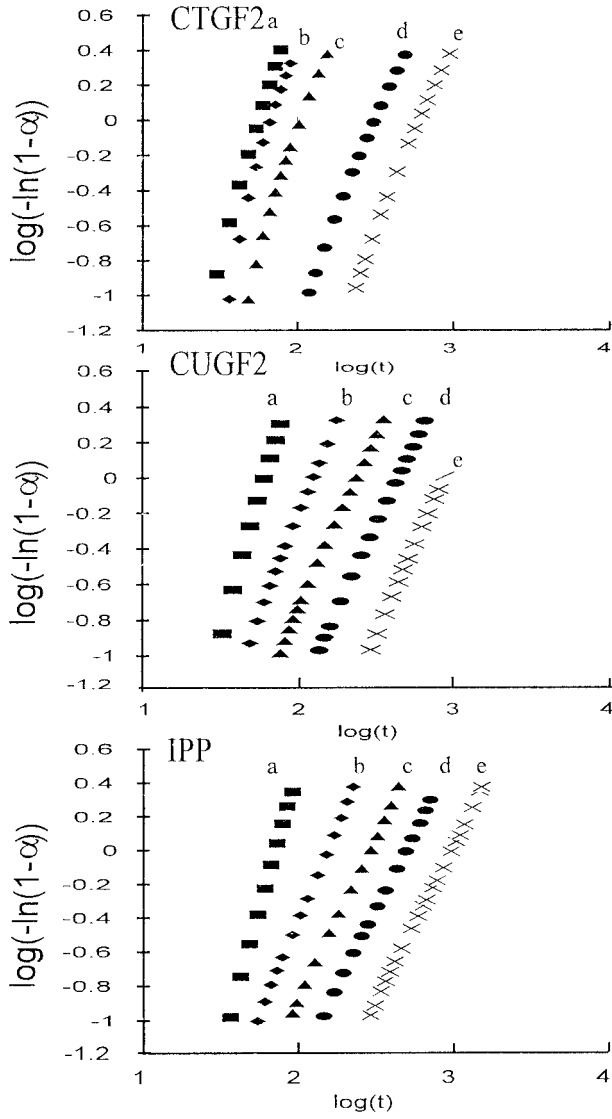


**Figure 3** Avrami plots for the system shown in Figure 2.

to a given crystallization temperature ( $T_c$ ) with cooling rate of 80 K/min. Isothermal crystallization is carried out at the  $T_c$  until crystallization was completed. The experiments were carried out with Perkin–Elmer DSC-7 analyzer under nitrogen, and the calibration was performed with indium and zinc. Based on the determined values for the enthalpy of crystallization, the extent of crystallization (crystal conversion),  $\alpha$ , is calculated:

$$\alpha = \int_0^t (dH/dt) dt / \int_0^\infty (dH/dt) dt \quad (1)$$

From the curves of  $\alpha$  against time, the induction period ( $t_i$ )<sup>18</sup> as well as the half-time of crystalliza-

**Table II** Avrami Exponents and Overall Crystallization Rates for Pure iPP and Model Composites at Different  $T_c$

$T_c$ (K)	iPP		CTGF2		CTGF3		CTGF5		CUGF2		CUGF3		CUGF5	
	$n$	$K$	$n$	$K$	$n$	$K$	$n$	$K$	$n$	$K$	$n$	$K$	$n$	$K$
388	4.4	$6.4 \times 10^{-7}$	3.0	$4.84 \times 10^{-6}$	3.3	$9.27 \times 10^{-7}$	3.1	$1.73 \times 10^{-6}$	3.3	$9.67 \times 10^{-7}$	3.2	$1.75 \times 10^{-6}$	3.3	$1.21 \times 10^{-6}$
391	2.2	$1.5 \times 10^{-5}$	3.2	$1.09 \times 10^{-6}$	2.4	$1.25 \times 10^{-6}$	2.3	$2.11 \times 10^{-5}$	2.3	$1.28 \times 10^{-5}$	2.1	$4.07 \times 10^{-5}$	2.4	$1.43 \times 10^{-5}$
394	2.0	$2.2 \times 10^{-5}$	2.6	$4.92 \times 10^{-5}$	2.2	$9.80 \times 10^{-6}$	2.2	$1.06 \times 10^{-5}$	2.0	$1.44 \times 10^{-5}$	2.0	$2.79 \times 10^{-5}$	2.1	$1.47 \times 10^{-5}$
397	2.0	$1.3 \times 10^{-5}$	2.1	$4.45 \times 10^{-6}$	2.2	$2.20 \times 10^{-6}$	2.1	$5.33 \times 10^{-6}$	2.0	$5.55 \times 10^{-6}$	1.8	$1.84 \times 10^{-5}$	2.0	$2.32 \times 10^{-6}$
400	1.9	$3.2 \times 10^{-6}$	2.1	$1.10 \times 10^{-6}$	2.1	$1.25 \times 10^{-6}$	2.1	$1.43 \times 10^{-6}$	2.8	$7.56 \times 10^{-9}$	2.1	$1.84 \times 10^{-5}$	2.0	$1.85 \times 10^{-6}$

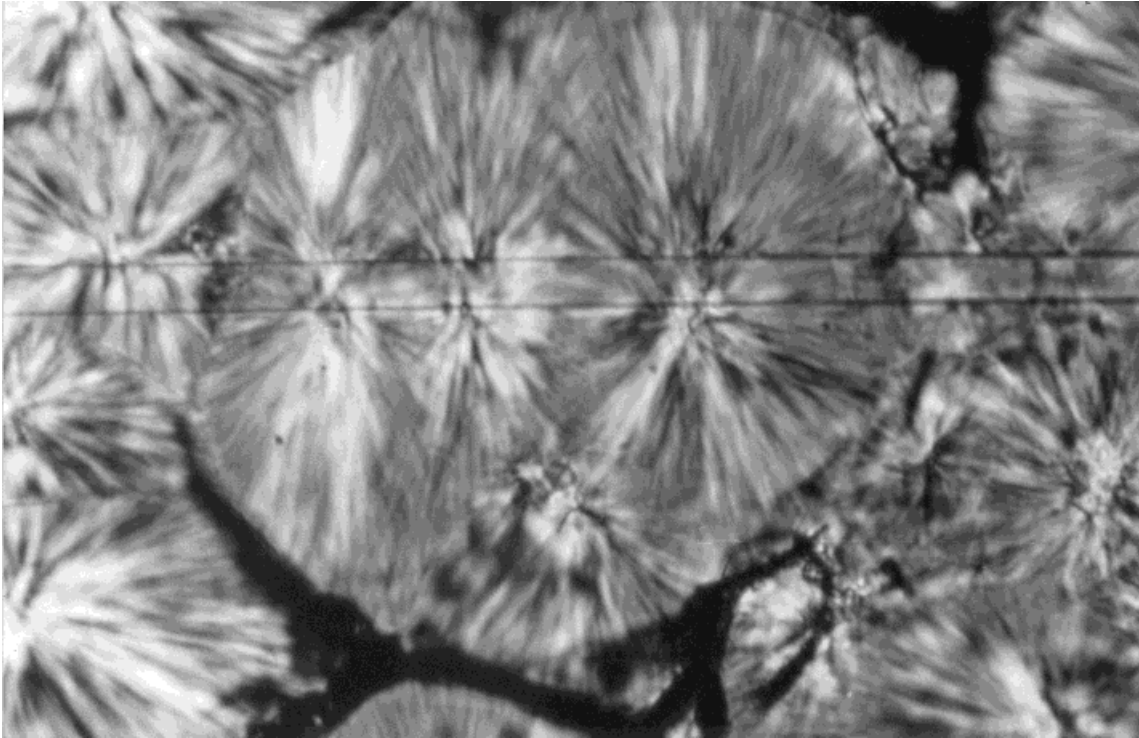


**Figure 4** Polarizing optical micrograph of iPP crystallized in the presence of TGF.

tion ( $t_{0.5}$ ) are determined as shown in Figure 1. Model iPP/glass-fiber composites were prepared with 20, 30, and 50 mass % of untreated unsized and thermally treated glass fibers, assigned as CGU and CGT, respectively, as presented in Table I.

## THEORETICAL BACKGROUND

From the DSC scans (isothermal crystallization at given  $T_c$  and then melting of the crystallized sample), the equilibrium melting temperature ( $T_m^0$ ) was determined by the Hoffman–Weeks method<sup>19</sup>:

$$T'_m = T_m^0(\gamma - 1)/\gamma + T_c/\gamma \quad (2)$$

where  $\gamma$  is a constant which represents the ratio between the final thickness of the crystalline lamellae and the initial critical thickness, and  $T'_m$  is the observed melting temperature of the sample isothermally crystallized at  $T_c$ .

According to the kinetic theory of polymer crystallization,<sup>20</sup> assuming that the lamellar growth controlled by a process of coherent two-dimensional surface (secondary) nucleation, the temperature dependence of  $k$  is given by the relation

$$\log(k)/n = A_0 - \Delta F^*/2.3RT_c - \Delta\Phi^*/2.3KT_c \quad (3)$$

where  $A_0$  is a constant (with the assumption that primary nucleation density at each  $T_c$  examined does not vary with time);  $\Delta F^*$ , the activation energy for the transport of crystallizing units across the liquid/solid interface; and  $\Delta\Phi^*$ , the energy of formation of a nucleus with critical dimensions, expressed as<sup>20</sup>:

$$\Delta\Phi^* = 4b_0\sigma\sigma_e T_m/\Delta H_f \Delta T \quad (4)$$

In this equation,  $b_0$  is the molecular thickness;  $\sigma$  and  $\sigma_e$ , the crystal growth lateral surface energy and the crystal fold surface energy, respectively;  $\Delta H_f$ , the enthalpy of fusion; and  $\Delta T = T_m^0 - T_c$ , supercooling.  $\Delta F^*$  is usually expressed as the activation energy of the viscous flow given by the Williams–Landell–Ferry relation<sup>21</sup>:

$$\Delta F^* = C_1 T_c / (C_2 + T_c - T_g) \quad (5)$$

where  $C_1$  and  $C_2$  are constants ( $C_1 = 17.2$  kJ/mol;  $C_2 = 51.5$  K) and  $T_g$  is the glass transition temperature. In further calculations, the literature value of  $T_g = 260$  K (ref. 22) was used for all model composites.

The plot [ $\log(k)/n + \Delta F^*/2.3RT_c$ ] versus

$T'_m/T_c\Delta T$  yields a straight line with the slope proportional to

$$4b_0\sigma\sigma_e/2.3K\Delta H_f \quad (6)$$

from which  $\Delta\Phi^*$  and  $\sigma_e$  are obtained assuming that  $b_0 = 0.525$  nm,<sup>22</sup>  $\Delta H_f = 209$  kJ/kg,<sup>23</sup> and  $\sigma = 0.1b_0H_f$ .

The  $T_m^0 = f(T'_m)$  relation is given by the Gibbs–Thompson equation<sup>24,25</sup>:

$$T'_m = T_m^0[1 - (2\sigma_e/\Delta H_u l)] \quad (7)$$

where  $l$  represents the lamellar thickness and  $\Delta H_u$  is the heat of fusion per unit volume of the polymer with 100% crystallinity ( $\Delta H_u = 1.99 \times 10^8$  J/m<sup>3</sup>).

The thickness of the critical crystal's coherent two-dimensional nucleus is given as<sup>24</sup>

$$l^* = 2\sigma_e/\Delta G_u \quad (8)$$

where  $\Delta G_u$  is the difference between free energy for the polymer melt and crystal and can be approximated by  $\Delta H_u\Delta T/T_m$ .

## RESULTS AND DISCUSSION

Based on DSC scans of isothermal crystallization (Fig. 2), crystal conversions were determined, and as evidenced from Figure 3, the plot  $\log[-\ln(1 - \alpha)]$  versus  $\log(t)$  yields a straight line, indicating that the kinetics of crystallization follows the Avrami equation<sup>26</sup>:

$$\log[-\ln(1 - \alpha)] = \log(k) + n \log(t) \quad (9)$$

The rate constant  $k$  and the Avrami exponent  $n$  were determined and the values are reported in Table II. A tendency of decreasing values of  $n$  with increasing  $T_c$  is found in the investigated interval of  $T_c$ . Also, at a constant but higher supercooling ( $T_c = 388$  K and  $T_c = 391$  K), the  $n$  value decreases with increasing glass fiber content. Transcrystallization was not observed in the vicinity of the fiber surface during the crystallization of iPP from the melt (Fig. 4).

DSC melting curves of the isothermally crystallized samples are shown in Figure 5. The equilibrium melting temperature of iPP in the composites is determined by the Hoffman–Weeks method, using the values of the maxima of low-temperature melting peaks. The value of  $T_m^0$

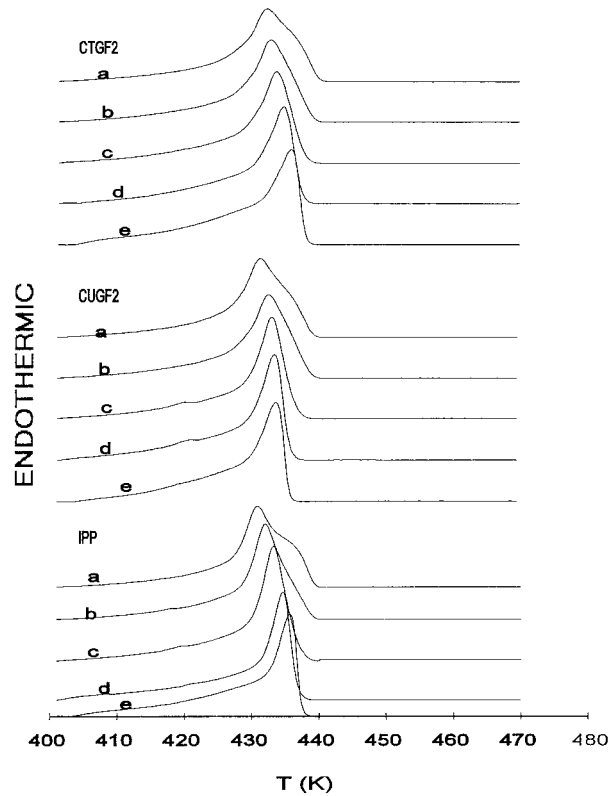


**Figure 5** DSC melting curves (heating rate: 10 K/min) of pure iPP and iPP in model composites after isothermal crystallization carried out at different temperatures— $T_c$ : (a) 388 K; (b) 391 K; (c) 394 K; (d) 397 K; (e) 400 K.

= 457 K is obtained and is close to the values presented for iPP in the literature.<sup>27</sup> It can be noticed from Table III that  $T_m^0$  decreases and the  $\gamma$  constant increases as the content of glass fibers in the model composites increase.

Different values for  $\sigma_e$  are determined for model composites containing 20–0.50% mass glass fibers, ranging from  $140$  to  $173 \times 10^{-3}$  J/m<sup>2</sup>, lower than  $\sigma_e = 178 \times 10^{-3}$  J/m<sup>2</sup> determined for pure iPP. Data for  $\sigma_e$  of iPP reported in the literature range from  $40 \times 10^{-3}$  J/m<sup>2</sup> (ref. 28) to  $230 \times 10^{-3}$  J/m<sup>2</sup>,<sup>29</sup> and the differences are usually related to different values of the constants used, including  $T_m^0$ .

Figures 6 and 7 show the induction time, which at a given  $T_c$  is defined as time for the formation of the equilibrium nucleus with critical dimensions<sup>18</sup> against the glass fiber content.  $t_i$  decreases as the fiber content increases, and this tendency also appears to be dependent on the thermal treatment of the fibers. At constant  $T_c$ ,  $t_i$  is lower for the composites containing treated as compared to unsized untreated glass fibers.

**Table III** Equilibrium Melting Temperature, Surface Free Energy of Folding, and  $\gamma$  Constants for Pure i-PP and Model Composites

GF (%)	CTGF				CUGF			
	$T_m$ (K)	$\sigma_e \times 10^3$ (J/m <sup>2</sup> )	$\gamma$	* $\gamma$	$T_m$ (K)	$\sigma_e \times 10^3$ (J/m <sup>2</sup> )	$\gamma$	* $\gamma$
0	457.13	178	2.67	2.70	457.13	178	2.67	2.70
20	451.60	147	3.24	3.30	453.77	157	2.94	2.98
30	454.30	158	3.06	3.10	456.87	172	2.70	2.73
50	451.24	140	3.36	3.42	453.42	151	3.26	3.29

\*  $\gamma = 1/\gamma^*$ .

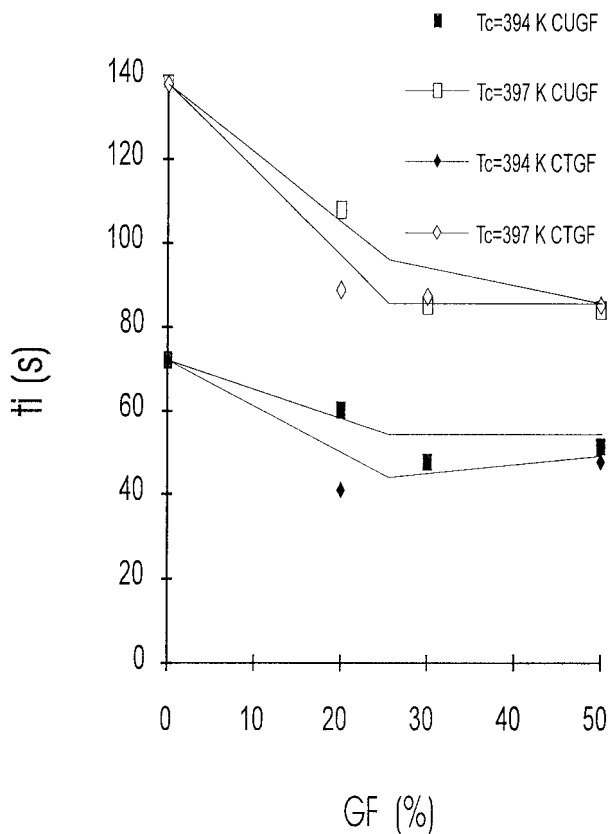
The crystallization rate constant depends on the half-time of crystallization and the overall crystallinity<sup>30</sup>:

$$k = \ln 2/t_{0.5}n \quad (10)$$

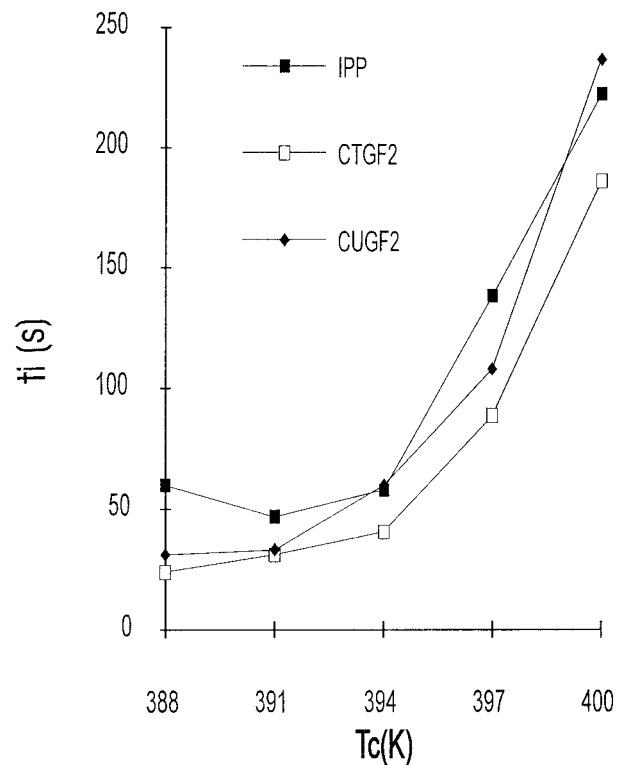
and is also related to the nucleation density ( $N$ ) and spherulite growth rate<sup>19</sup>:

$$k = 4\pi\rho_c G^3 N / 3\rho_a(1 - \alpha_\infty) \quad (11)$$

$$N = N_0 \exp(-\Delta\Phi/2.3KT + \Delta F/2.3RT) \quad (12)$$

**Figure 6** Induction time versus glass-fiber content.

In our previous examinations based on polarizing optical microscopy<sup>31</sup> it was shown that the spherulitic growth rate is practically unchanged and similar for iPP and the model composites. In the temperature range investigated ( $T_c = 389$ – $409$  K), the values of  $0.5$ – $4.7$   $\mu\text{m}/\text{min}$  for  $G$  were determined and are constant at a given  $T_c$ . The half-time of crystallization  $t_{0.5}$  for iPP and the model composites as a function of  $T_c$  and the glass fiber content is shown in Figures 8 and 9, respectively. The values of  $t_{0.5}$  for composites containing treated glass fibers are lower than for pure iPP and the composites with untreated glass fibers for

**Figure 7** Induction time of crystallization versus  $T_c$ .

a given  $T_c$ . Also,  $t_{0.5}$  for a given  $T_c$  decreases with an increase of the glass fiber content, which is in agreement with eqs. (10) and (11):  $t_{0.5}$  decreases ( $k$  increase) as the nucleation density increases if  $G$  is approximately constant.<sup>9</sup> The observed differences between the composites containing untreated and treated glass fibers might be attributed obviously to the predominant nucleating effect of treated fibers. A similar trend is found for  $t_i$ , thus pointing out that the overall kinetic rate constant  $k$  depends on the rate of nucleation.

The energy of formation of a nucleus of critical dimension at given  $T_c$  is lower for the composites compared to pure iPP and decreases as the content of glass fibers in the model composites increases (Figs. 10 and 11). The effect of the fiber's thermal treatment is again evident, since in the case of treated fibers, the lowest values of  $\Delta\Phi^*$  are obtained at each  $T_c$  and each  $W_{gf}$ .

The values for critical thickness  $l^*$  against  $T_c$  are shown in Figure 12. Based on these results, a conclusion can be derived that better thermodynamic conditions are reached when treated fibers

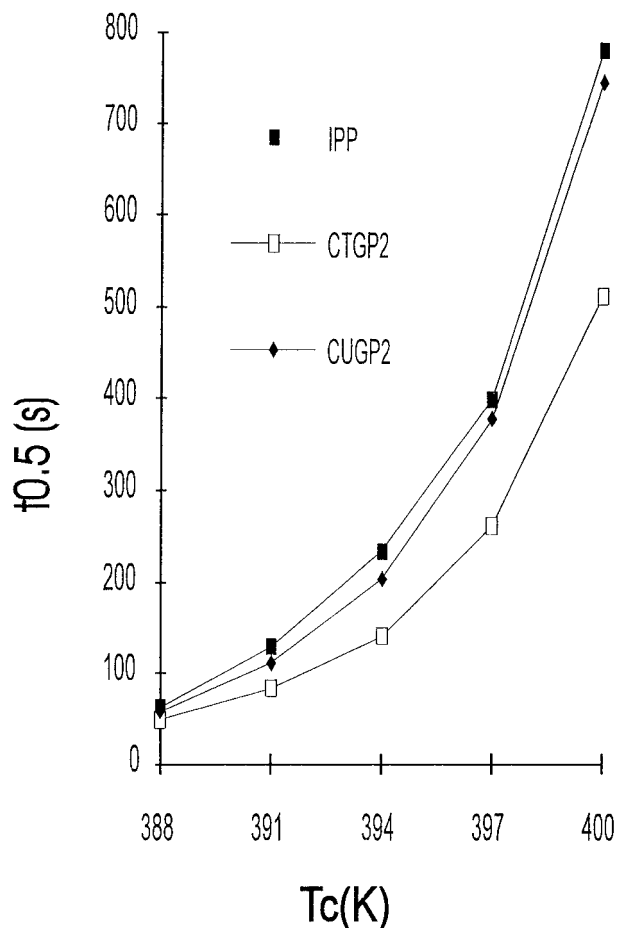


Figure 8 Half-time of crystallization versus  $T_c$ .

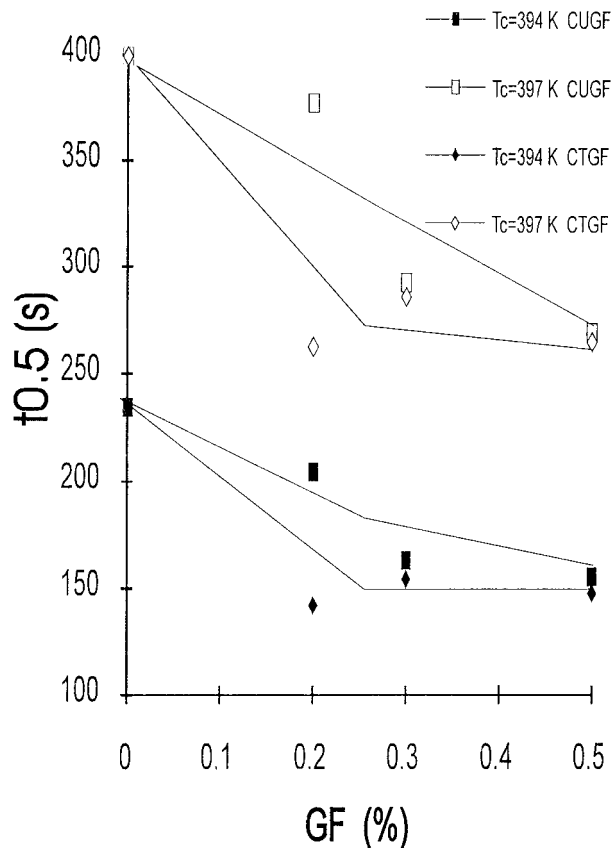


Figure 9 Half-time of crystallization versus glass-fiber content.

are used for the preparation of model composites. The results for  $\gamma$  determined by the Hoffman-Weeks method and from eqs. (7) and (8) ( $\gamma^*$ ) are summarized in Table III. The differences between  $\gamma$  and  $\gamma^*$  are within  $10^{-2}$ , pointing out the significance of the equations used for calculating  $l^*$ .

## CONCLUSION

A quantitative approach based on the theory of the crystallization of polymers, enabling the determination of the basic energetic parameters of iPP/glass-fiber model composites is presented. It was shown that in the presence of glass fibers isothermal crystallization of iPP occurred faster, and the values of  $t_i$  and  $t_{0.5}$  were lowest for composites containing treated fibers. During the isothermal crystallization of iPP in the presence of fibers, the crystalline lamellar thickness increased as the fiber content increased. Thermally treated glass fibers are found to exhibit a predominant nucleating effect as compared to untreated

unsized fibers. The energy of formation of a nucleus of critical dimensions at given  $T_c$  is also lower in the presence of fibers, and it decreases as the content of fibers in the composite increases. For the composites containing 50% TGF glass fibers, the value of  $\sigma_e = 140 \times 10^{-3} \text{ J/m}^2$  was determined, while for the pure iPP matrix,  $\sigma_e$  is  $178 \times 10^{-3} \text{ J/m}^2$ .

**NOMENCLATURE LIST OF SYMBOLS**

- $T_m^0$  equilibrium melting temperature
- $T_m'$  observed melting temperature of the sample
- $T_g$  the glass transition temperature
- $\Delta T$  supercooling
- $t_i$  incubation time
- $t_{0.5}$  half time of crystallization
- $\gamma$  constant which represents the ratio between the final thickness of the crystalline lamellae and the initial critical thickness

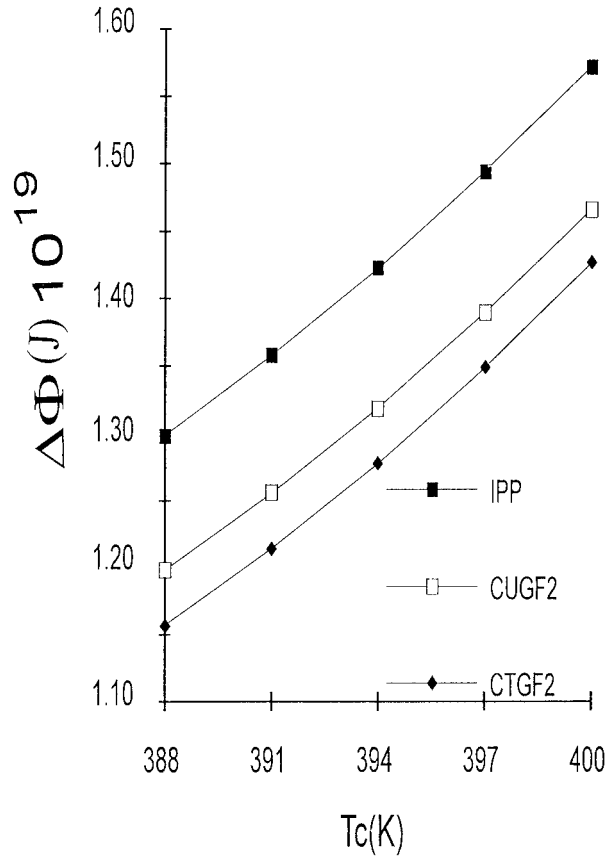


**Figure 10** Energy of formation of nucleus of critical dimensions versus  $T_c$ .

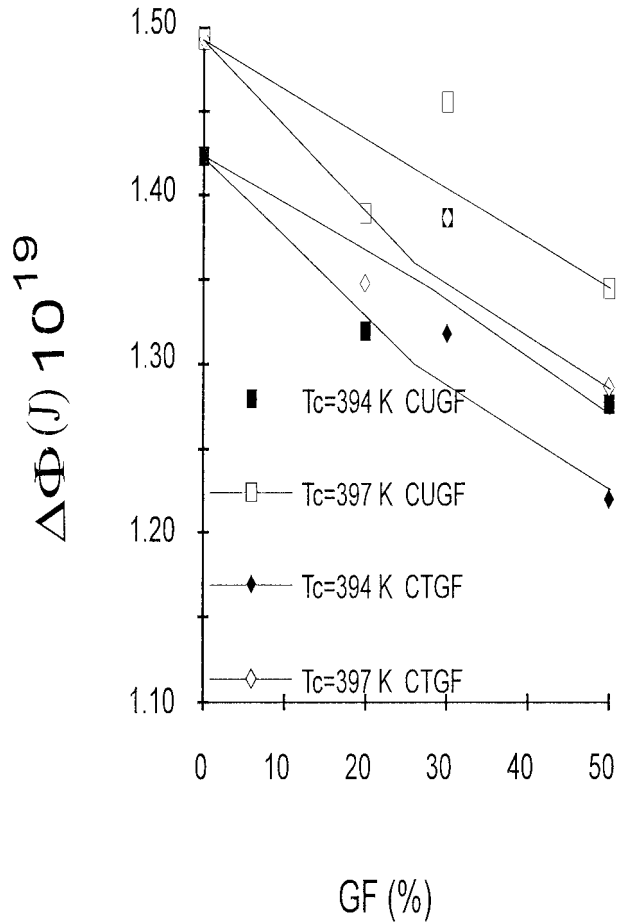


**Figure 11** Energy of formation of nucleus of critical dimensions versus glass fiber content.

- $A_0$  constant
- $\Delta F^*$  activation energy for the transport of crystallizing units across the liquid/solid interface
- $\Delta \Phi^*$  energy of formation of a nucleus with critical dimensions
- $\sigma$  crystal growth lateral surface energy
- $\sigma_e$  crystal fold surface energy
- $\Delta H_f$  enthalpy of fusion
- $k$  rate constant
- $n$  Avrami coefficient
- $R$  universal gas constant
- $K$  Boltzman constant constant
- $b_0$  molecular thickness
- $C_1$  and  $C_2$  constants
- $l$  lamellae thickness
- $l^*$  critical thickness of the crystal' coherent two-dimensional nucleus
- $\Delta H_u$  the heat of fusion per unit volume
- $\Delta H_f$  heat of fusion



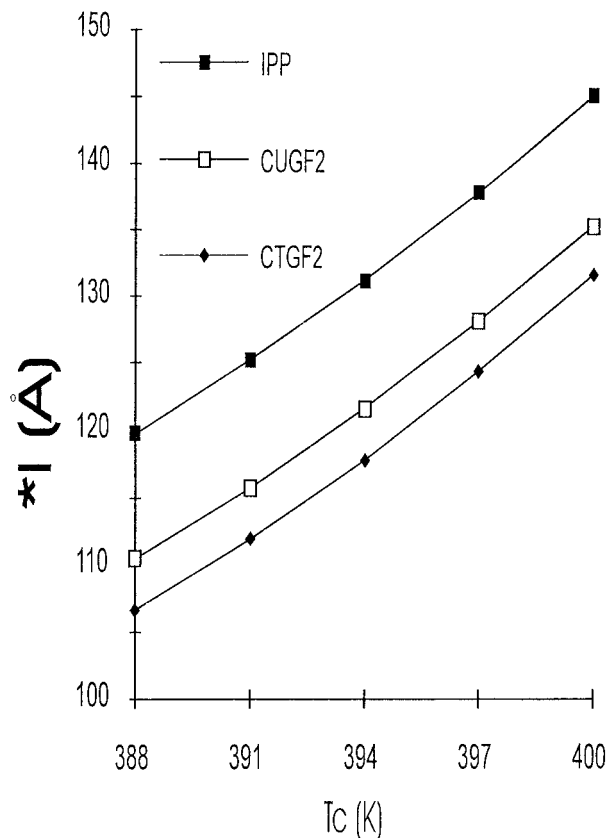


**Figure 12** Thickness of the critical nucleus versus  $T_c$ .

$\Delta G_u$	is the difference between free energy for polymer melt and crystal
$N$	nucleation density
$G$	spherulite growth rate
$\rho_c$	crystal density
$\rho_a$	amorphous density
$\alpha$	crystal conversion

## REFERENCES

1. T. W. Chou, Ed., *Materials Science and Technology*, vol. 13, VCH, Weinheim, 1993.
2. B. Wunderlich, *Macromolecular Physics*, Vol. 2, Academic Press, New York, 1976, Chap. 5.
3. E. Devaux and B. Chabert, in *II IPCM Conference Proceedings*, Leuven, Belgium, Sept. 1991, pp. 115–118, 17–19.
4. F. Hoecker and J. Karger-Kocsis, *J. Adhes.*, **52**, 81 (1995).
5. N. Billon, C. Magnet, J. M. Haudin, and D. Lefebvre, *Colloid Polym. Sci.*, **272**, 633 (1994).
6. D. G. Gray, *J. Polym. Sci. Polym. Lett. Ed.*, **2**, 509 (1974).
7. D. Campbell and M. M. Qayyum, *J. Mater. Sci.*, **12**, 2427 (1977).
8. J. L. Thomason and A. A. Von Rooyen, *J. Mater. Sci.*, **27**, 889 (1992).
9. M. Avela, E. Martuscelli, C. Sellitt, and E. Garagnani, *J. Mater. Sci.*, **22**, 3185 (1987).
10. F. Rybnikar, *J. Appl. Polym. Sci.*, **27**, 1479 (1982).
11. J. Menzel and J. Varga, *J. Therm. Anal.*, **28**, 161 (1983).
12. D. Campbell and M. M. Qayyum, *J. Polym. Sci. Polym. Phys. Ed.*, **18**, 83 (1980).
13. J. Varga and J. Karger-Kocsis, *Polym. Bull.*, **30**, 105 (1993).
14. J. Devaux and B. Chabert, *Polym. Commun.*, **31**, 391 (1990).
15. G. Dembovski, A. Grozdanov, K. Ljapceva, G. Bogoeva-Gaceva, and B. Mangovska, *Textiles*, **45**, 11 (1996).
16. G. Bogoeva-Gaceva, A. Janevski, and A. Grozdanov, *J. Appl. Polym. Sci.*, **67**, 395 (1998).
17. A. Kelly and Yu. N. Rabotonov, *Handbook of Composites*, Vol. 1, Elsevier, Amsterdam, 1985, p. 23.
18. Y. Long, R. A. Shanks, and Z. H. Stachurski, *Prog. Polym. Sci.*, **20**, 651 (1995).
19. J. D. Hoffman, *Soc. Plast. Eng. Trans.*, **4**, 315 (1964).
20. J. D. Hoffman, G. T. Davis, and S. I. Lauritzen, in *Treatise on Solid State Chemistry*, Vol. 3, N. B. Hannay, Ed., Plenum, New York, 1976, Chap. 7.
21. H. L. Williams, R. F. Landel, and J. D. S. Ferry, *J. Am. Chem. Soc.*, **77**, 3701 (1955).
22. L. Grispino, E. Martuscelli, and M. Pracella, *Z. Macromol. Chem.*, **181**, 1747 (1980).
23. S. Brandup and E. H. Immergut, *Polymer Handbook*, Vol. 5, Interscience, New York, 1975, p. 24.
24. J. W. Gibbs, *The Scientific Work of J. Willard Gibbs*, Vol. 1, Longmans Green, New York, 1906.
25. J. J. Thompson, *Applications of Dynamic*, Macmillan, London, 1988.
26. M. Avrami, *J. Chem. Phys.*, **9**, 177 (1941).
27. J. J. Janimak, S. Z. D. Cheng, and A. Zhang, *Polymer*, **33**, 728 (1992).
28. K. Godowsky and G. L. Slovonimsky, *J. Polym. Sci.*, **12**, 1053 (1974).
29. E. Martuscelli, C. Silvestre, and G. Abote, *Polymer*, **23**, 229 (1982).
30. L. Mandelkeren, *Crystallization Polymer*, McGraw-Hill, New York, 1964.
31. A. Grozdanov and G. Bogoeva-Gaceva, *J. Serb. Chem. Soc.*, submitted.